Structural Damage Measure Index Based on Non-probabilistic Reliability Model

Xiaojun Wang[a,b], Yong Xia[a†], Xiaoqing Zhou[c], Chen Yang[b]

[a] *Department of Civil and Environmental Engineering, The Hong Kong Polytechnic University, Hung Hom, Hong Kong, China*

[b] *Institute of Solid Mechanics, Beihang University, Beijing 100191, China*

[c] *College of Civil Engineering, Shenzhen University, Shenzhen 518060, China*

ABSTRACT

Uncertainties in the structural model and measurement data affect structural condition assessment in practice. As the probabilistic information of these uncertainties lacks, the non-probabilistic interval analysis framework is developed to quantify the interval of the structural element stiffness parameters. According to the interval intersection of the element stiffness parameters in the undamaged and damaged states, the possibility of damage existence is defined based on the reliability theory. A damage measure index is then proposed as the product of the nominal stiffness reduction and the defined possibility of damage existence. This new index simultaneously reflects the damage severity and possibility of damage at each structural component. Numerical and experimental examples are presented to illustrate the validity and applicability of the method. The results show that the proposed method can improve the accuracy of damage diagnosis compared with the deterministic damage identification method.

Keywords: damage identification, uncertainty, interval analysis, non-probabilistic reliability model

[†] Corresponding author, Associate Professor, e-mail: ceyxia@polyu.edu.hk, Tel: +852-27666066

1. Introduction

Within their service lives, civil structures are inevitably subjected to deterioration and damage resulting from environmental erosion, overloading, fatigue, material aging, or other unexpected factors. Damage detection at the possible earliest stage pervades in the civil, mechanical, and aerospace engineering communities [1]. Because of the limitations in experimental methods, where the vicinity of the damage must be known a priori and the portion of the structure being inspected must be readily accessible, vibration-based damage detection methods have been developed extensively since the 1990s [2].

The dynamic properties of the frequency domain (such as natural frequency, mode shape, mode shape curvature, modal flexibility, and modal strain energy) [3-6] or the responses in the time domain [7-9] have been adopted as indicators of damage. In practice, measurement data are always limited and contain noises or errors to some extent. To reduce the effects of the uncertainty of limited measurement data on the damage diagnosis, researchers are searching for indicators with high sensitivity to damage so that the useful information is not drowned by the noises [10]. On the other hand, statistical damage identification methods have been proposed to address various uncertainties involved [11].

Collins et al. [12] first derived a statistical identification procedure by treating the initial structural parameters as normally distributed random variables with zero means and specific covariance. Xia and Hao [13] developed a statistical damage identification algorithm accounting for the effects of measurement noise in the natural frequencies and variations in the finite element (FE) model, and derived the probability of damage existence. They further extended the statistical approach to the case with combined frequency and mode shape data for structural damage identification [14]. Based on acceleration responses, Li and Law [15] analyzed the influence of the uncertainty of system parameters and the measurement data on damage identification. Yeo et al. [16] presented a damage assessment algorithm for framed structures using static responses with a regularization technique, in which statistical distributions of the system parameters with a set of noise-polluted measurement data were derived by the perturbation method and then the damage was assessed by a statistical hypothesis test approach. To avoid damage identification induced by the measurement noise, a probabilistic method was proposed to identify the structural damages with uncertainties under unknown input [17].

In these methods, the statistical distributions of the uncertainties are assumed to be known (usually as Gaussian distribution). In practice, however, the uncertainty sources are complicated, and experimental data under a particular condition are insufficient. The probabilistic distributions of the uncertainties are usually not available. In this regard, the non-probabilistic interval analysis has been developed [18, 19] for damage identification, in which the uncertainty bounds, rather than the probabilistic distributions, of the measurement data are employed. Wang et al. [20, 21] applied the interval analysis technique for structural damage identification using the bounded natural frequencies and the static displacements of the structures, respectively. Damage identifications for a steel cantilever beam and a steel cantilever plate were performed by the proposed non-probabilistic method in comparison with the probabilistic approach [20].

In both probabilistic and non-probabilistic approaches, the nominal (or mean value of) stiffness reduction of each element and the probability (or possibility) of damage are separately provided to assess the damage of the structures. However, a significant stiffness reduction may have a low probability of damage because probability is associated with both the mean value and the variance. For the same reason, a small stiffness reduction may have a relatively high probability. Therefore, using the mean value of the stiffness reduction or the probability of damage alone may not come up with an accurate damage assessment.

In this paper, the stiffness reduction and possibility of damage are combined as a new damage measure index (DMI). The non-probabilistic interval analysis framework is adopted to identify the stiffness parameter interval from the measured uncertain frequencies and mode shapes. The possibility of damage of each structural member is calculated by virtue of the non-probabilistic, set-theoretic reliability theory [22] from the member stiffness intervals in the undamaged and damaged states. The DMI is defined as the product of the nominal stiffness reduction and possibility of damage. It simultaneously reflects the degree and possibility of damage for each structural component. A numerical example of a 15-bar truss structure and an experimental example of a one-span steel portal frame are presented to demonstrate the effectiveness of the proposed method.

2. Deterministic FE model updating using both frequencies and mode shapes

The free vibration problem of an undamped structure with N degrees of freedom can be expressed as

$$\mathbf{K}\boldsymbol{\phi}_i = \lambda_i \mathbf{M}\boldsymbol{\phi}_i \,, \quad i = 1, 2, ..., N \tag{1}$$

where $\mathbf{M}$ is the $N \times N$ mass matrix, $\mathbf{K}$ is the $N \times N$ stiffness matrix, $\mathbf{x}(t)$ and $\ddot{\mathbf{x}}(t)$ are the displacement and acceleration vectors, respectively, and λ_i and $\boldsymbol{\phi}_i$ are the *i*th eigenvalue and mass-normalized mode shape, respectively. If changes occur in the structural parameters, the eigenvalue problem is expressed as

$$\mathbf{K}_c\boldsymbol{\phi}_{ci} = \lambda_{ci} \mathbf{M}_c\boldsymbol{\phi}_{ci} \,, \quad i = 1, 2, ..., N \tag{2}$$

where $\mathbf{K}_c$, $\mathbf{M}_c$, λ_{ci}, and $\boldsymbol{\phi}_{ci}$ are the corresponding quantities in the changed state.

For the FE model of the structure, $\mathbf{K}$ can be expressed in the following non-negative parameter decomposition form:

$$\mathbf{K} = \sum_{i=1}^{m} \alpha_i \mathbf{K}_i = \alpha_1 \mathbf{K}_1 + \alpha_2 \mathbf{K}_2 + ... + \alpha_m \mathbf{K}_m \tag{3}$$

where m is the number of elements in the structure, α_i is the initial elemental stiffness parameter (ESP), and $\mathbf{K}_i$ is the *i*th element stiffness matrix divided by α_i. Similarly, $\mathbf{K}_c$ is set up as

$$\mathbf{K}_c = \sum_{i=1}^{m} \alpha_{ci} \mathbf{K}_i = \alpha_{c1} \mathbf{K}_1 + \alpha_{c2} \mathbf{K}_2 + ... + \alpha_{cm} \mathbf{K}_m \,. \tag{4}$$

The model updating is based on the relationship between the measured vibration characteristics and the ESP using the first-order Taylor series expansion as [12]

$$\begin{pmatrix} \boldsymbol{\lambda}_c \\ \boldsymbol{\phi}_c \end{pmatrix} = \begin{pmatrix} \boldsymbol{\lambda} \\ \boldsymbol{\phi} \end{pmatrix} + \mathbf{S}\left(\boldsymbol{\alpha}_c - \boldsymbol{\alpha}\right) \tag{5}$$

where $\mathbf{S}$ is the sensitivity matrix of the modal properties with respect to the ESPs [23].

When the natural frequencies and mode shapes of the initial and changed structures are available, ESP changes $\Delta\boldsymbol{\alpha} = \boldsymbol{\alpha}_c - \boldsymbol{\alpha}$ can be derived by solving the following equation [14]:

$$\mathbf{S}\Delta\boldsymbol{\alpha} = \Delta\mathbf{e} \tag{6}$$

where $\Delta\mathbf{e} = \begin{pmatrix} \boldsymbol{\lambda}_c - \boldsymbol{\lambda} \\ \boldsymbol{\phi}_c - \boldsymbol{\phi} \end{pmatrix}$ is the modal data change vector containing the differences of the eigenvalues and mode shapes. Assume that the mode shapes are measured at np degrees of freedom of the structure and the number of available modes is nm in the initial and changed states. Consequently $\Delta\mathbf{e}$ has a length of $nm\times(1+np)$. Because the degrees of accuracy of the measured vibration frequencies and mode shapes are different, different weights can be assigned to the frequencies and mode shapes in vector $\Delta\mathbf{e}$ [24].

The least square solution to Eq. (6) is

$$\Delta\boldsymbol{\alpha} = \mathbf{S}^{+}\Delta\mathbf{e} \tag{7}$$

where $\mathbf{S}^{+}$ is the Moore–Penrose generalized inverse of matrix $\mathbf{S}$. As high-order terms are neglected in Eq. (6), an iterative computation or optimization procedure for Eq. (7) can be employed [24].

Based on the above model updating procedure, the ESPs before and after the damage can be obtained using the measured modal data in the undamaged and damaged states, respectively. The elemental stiffness reduction factor (SRF) is calculated as the change of ESP to the initial value as

$$\mathrm{SRF}_i = \Delta\alpha_i / \alpha_{ui} = \left(\alpha_{di} - \alpha_{ui}\right) / \alpha_{ui} \tag{8}$$

where subscripts "u" and "d" represent the updated ESP values in the undamaged and damaged states, respectively.

3. Identification of interval for ESPs

In this section, the interval-based parameter identification that considers uncertain measurements and modelling is proposed. If the uncertainty level is larger than or close to the frequency changes due to damages, the damage cannot be correctly identified and the healthy members may be falsely identified as damaged.

Based on the interval mathematics, the intervals of the analytical ESPs, eigenvalues, and mode shapes in the undamaged or damaged state can be expressed as

$$\boldsymbol{\alpha}^I = [\underline{\boldsymbol{\alpha}}, \overline{\boldsymbol{\alpha}}] = \left\{a_1^I, \alpha_2^I, \cdots, \alpha_m^I\right\}^T, \quad \alpha_i^I = \left[\underline{\alpha_i}, \overline{\alpha_i}\right], \quad i = 1, 2, \ldots, m \tag{9}$$

$$\boldsymbol{\lambda}_c^I = \left[\underline{\boldsymbol{\lambda}_c}, \overline{\boldsymbol{\lambda}_c}\right] = \left\{\lambda_{c1}^I, \lambda_{c2}^I, \ldots, \lambda_{cnm}^I\right\}^T, \quad \lambda_{ci}^I = \left[\underline{\lambda_{ci}}, \overline{\lambda_{ci}}\right], \quad i = 1, 2, \ldots, nm \tag{10}$$

$$\boldsymbol{\phi}_c^I = \left[\underline{\boldsymbol{\phi}_c}, \overline{\boldsymbol{\phi}_c}\right] = \left\{\left(\boldsymbol{\phi}_{c1}^I\right)^T, \left(\boldsymbol{\phi}_{c2}^I\right)^T, \ldots, \left(\boldsymbol{\phi}_{cnm}^I\right)^T\right\}^T, \quad \boldsymbol{\phi}_{ci}^I = \left[\underline{\boldsymbol{\phi}_{ci}}, \overline{\boldsymbol{\phi}_{ci}}\right], \quad i = 1, 2, \ldots, nm \tag{11}$$

where variables with underline and upper bar denote the lower and upper bounds of the variables, respectively.

The modelling errors can be reduced by a two-step model updating procedure [13, 20]. In each model updating step, the measurement uncertainties are the main factors that affect the parameter identification results because the updated ESPs are more sensitive to measurement uncertainties than to the FE modelling errors [13]. Note that the modelling errors are not only due to uncertainty of the model parameters but also the assumptions adopted in the modelling. This type of uncertainty is, however, difficult to quantify and not included in this study.

In practice, the lower and upper bounds of the modal parameters can be determined from repeated experimental modal data. By use of these experimental data, the mean value and standard deviation can be obtained. According to the Tchebycheff's inequality [25], the probability of the uncertain variable with finite variance falling within k standard deviation of its mean is at least $1-1/k^2$, and the bound is independent of the distribution of the uncertain variable. For a sufficient large k, an interval of the mean value plus and minus k times standard deviation will result in a certain event. ESP is associated with material properties and structural component dimensions, whose statistical properties can be found in literature. For example, Reference 26 has reported the statistical properties of material modulus and dimensions in various practical common structures.

The middle value and the radius of the interval variables are introduced as

$$\mathbf{x}^c = \mathrm{m}\left(\mathbf{x}^I\right) = \left(\underline{\mathbf{x}} + \overline{\mathbf{x}}\right)/2 \tag{12}$$

$$\Delta\mathbf{x} = \mathrm{rad}\left(\mathbf{x}^I\right) = \left(\overline{\mathbf{x}} - \underline{\mathbf{x}}\right)/2 \tag{13}$$

where $\mathbf{x}^c$ and $\Delta\mathbf{x}$ are the middle value and the radius (or uncertainty) of $\mathbf{x}^I$, respectively. For simplicity, α_i, λ_{ci}, and $\boldsymbol{\phi}_{ci}$ are written together as vector $\mathbf{X}$. Therefore, the uncertain parameters can be rewritten in the following form:

$$\begin{cases} \mathbf{X} = \mathbf{X}^c + \delta\mathbf{X} \quad , \quad \left|\delta\mathbf{X}\right| \le \Delta\mathbf{X} \\ X_i = X_i^c + \delta X_i \quad , \quad \left|\delta X_i\right| \le \Delta X_i \quad , \quad i = 1, 2, \ldots, nv \end{cases} \tag{14}$$

where $nv = m + nm + nm \times np$ is the number of uncertain interval variables, including m ESPs, nm eigenvalues, and nm mode shape vectors measured at np points.

According to the expression of the interval mathematics [20], the uncertain interval variables can be written as

$$\mathbf{X}^I = \left[\underline{\mathbf{X}}, \overline{\mathbf{X}}\right] = \mathbf{X}^c + \Delta\mathbf{X}^I = \mathbf{X}^c + \Delta\mathbf{X}\left[-1,1\right] = \mathbf{X}^c + \Delta\mathbf{X}e_\Delta$$

$$\mathbf{X}^c = \left\{X_1^c, X_2^c, ..., X_{nv}^c\right\}^T, \quad \Delta\mathbf{X} = \left\{\Delta X_1, \Delta X_2, ..., \Delta X_{nv}\right\}^T \tag{15}$$

where $e_\Delta = \left[-1,1\right]$. The degree of uncertainty for the interval variable is defined as

$$\xi_i = \Delta X_i / X_i^c . \tag{16}$$

In Eq. (6), vectors $\Delta\boldsymbol{\alpha}$ and $\Delta\mathbf{e}$ and matrix $\mathbf{S}$ are functions of $\mathbf{X} = \left(X_1, X_2, ..., X_{nv}\right)^T$.They can be written as

$$\Delta\boldsymbol{\alpha} = \Delta\boldsymbol{\alpha}\left(\mathbf{X}\right) = \left\{\Delta\alpha_1\left(\mathbf{X}\right), \Delta\alpha_2\left(\mathbf{X}\right), ..., \Delta\alpha_m\left(\mathbf{X}\right)\right\}^T \tag{17}$$

$$\Delta\mathbf{e} = \Delta\mathbf{e}\left(\mathbf{X}\right) = \left\{\Delta e_1\left(\mathbf{X}\right), \Delta e_2\left(\mathbf{X}\right), ..., \Delta e_{nmd}\left(\mathbf{X}\right)\right\}^T \tag{18}$$

$$\mathbf{S} = \mathbf{S}\left(\mathbf{X}\right) = \left(S_{ij}\left(\mathbf{X}\right)\right)_{nmd\times m} \tag{19}$$

where $nmd = nm + nm \times np$ is the length of the modal data vector.

Expanding Eqs. (17)–(19) as the first-order Taylor series in terms of X_i, we have

$$\Delta\boldsymbol{\alpha}\left(\mathbf{X}\right) = \Delta\boldsymbol{\alpha}\left(\mathbf{X}^c + \delta\mathbf{X}\right) \approx \Delta\boldsymbol{\alpha}\left(\mathbf{X}^c\right) + \sum_{i=1}^{nv} \frac{\partial\Delta\boldsymbol{\alpha}\left(\mathbf{X}^c\right)}{\partial X_i}\delta X_i \tag{20}$$

$$\Delta\mathbf{e}\left(\mathbf{X}\right) = \Delta\mathbf{e}\left(\mathbf{X}^c + \delta\mathbf{X}\right) \approx \Delta\mathbf{e}\left(\mathbf{X}^c\right) + \sum_{i=1}^{nv} \frac{\partial\Delta\mathbf{e}\left(\mathbf{X}^c\right)}{\partial X_i}\delta X_i \tag{21}$$

$$\mathbf{S}\left(\mathbf{X}\right) = \mathbf{S}\left(\mathbf{X}^c + \delta\mathbf{X}\right) \approx \mathbf{S}\left(\mathbf{X}^c\right) + \sum_{i=1}^{nv} \frac{\partial\mathbf{S}\left(\mathbf{X}^c\right)}{\partial X_i}\delta X_i \tag{22}$$

By substituting Eqs. (20)–(22) into Eq. (6) and neglecting the high-order terms, the following equations can be obtained:

$$\Delta\boldsymbol{\alpha}\left(\mathbf{X}^c\right) = \mathbf{S}\left(\mathbf{X}^c\right)^+ \cdot \Delta\mathbf{e}\left(\mathbf{X}^c\right) \tag{23}$$

$$\sum_{i=1}^{nv} \frac{\partial\Delta\boldsymbol{\alpha}\left(\mathbf{X}^c\right)}{\partial X_i}\delta X_i = \mathbf{S}\left(\mathbf{X}^c\right)^+ \sum_{i=1}^{nv}\left(\frac{\partial\Delta\mathbf{e}\left(\mathbf{X}^c\right)}{\partial X_i} - \frac{\partial\mathbf{S}\left(\mathbf{X}^c\right)}{\partial X_i}\cdot\Delta\boldsymbol{\alpha}\left(\mathbf{X}^c\right)\right)\delta X_i \tag{24}$$

where $\delta X_i \in \Delta X_i^I = \left[-\Delta X_i, \Delta X_i\right]$. Substitution of Eqs. (23) and (24) into Eq. (20) yields the expression of $\Delta\boldsymbol{\alpha}$ as

$$\Delta\boldsymbol{\alpha}\left(\mathbf{X}\right) = \mathbf{S}\left(\mathbf{X}^c\right)^+ \cdot \Delta\mathbf{e}\left(\mathbf{X}^c\right) + \mathbf{S}\left(\mathbf{X}^c\right)^+ \sum_{i=1}^{nv}\left(\frac{\partial\Delta\mathbf{e}\left(\mathbf{X}^c\right)}{\partial X_i} - \frac{\partial\mathbf{S}\left(\mathbf{X}^c\right)}{\partial X_i}\cdot\Delta\boldsymbol{\alpha}\left(\mathbf{X}^c\right)\right)\delta X_i . \tag{25}$$

Using the natural interval extension [20], we can obtain the interval of the ESP changes (i.e., $\Delta\boldsymbol{\alpha}$)

$$\Delta\boldsymbol{\alpha}^I\left(\mathbf{X}\right)=\mathbf{S}\left(\mathbf{X}^c\right)^+\cdot\Delta\mathbf{e}\left(\mathbf{X}^c\right)+\sum_{i=1}^{nv}\mathbf{S}\left(\mathbf{X}^c\right)^+\left(\frac{\partial\Delta\mathbf{e}\left(\mathbf{X}^c\right)}{\partial X_i}-\frac{\partial\mathbf{S}\left(\mathbf{X}^c\right)}{\partial X_i}\cdot\Delta\boldsymbol{\alpha}\left(\mathbf{X}^c\right)\right)\cdot\Delta X_i^I\,. \tag{26}$$

The lower and upper bounds of interval vector $\Delta\boldsymbol{\alpha}^I$ are

$$\underline{\Delta\boldsymbol{\alpha}\left(\mathbf{X}\right)}=\mathbf{S}\left(\mathbf{X}^c\right)^+\cdot\Delta\mathbf{e}\left(\mathbf{X}^c\right)-\sum_{i=1}^{nv}\left|\mathbf{S}\left(\mathbf{X}^c\right)^+\left(\frac{\partial\Delta\mathbf{e}\left(\mathbf{X}^c\right)}{\partial X_i}-\frac{\partial\mathbf{S}\left(\mathbf{X}^c\right)}{\partial X_i}\cdot\Delta\boldsymbol{\alpha}\left(\mathbf{X}^c\right)\right)\right|\cdot\Delta X_i \tag{27}$$

$$\overline{\Delta\boldsymbol{\alpha}(\mathbf{X})}=\mathbf{S}\left(\mathbf{X}^c\right)^+\cdot\Delta\mathbf{e}\left(\mathbf{X}^c\right)+\sum_{i=1}^{nv}\left|\mathbf{S}\left(\mathbf{X}^c\right)^+\left(\frac{\partial\Delta\mathbf{e}\left(\mathbf{X}^c\right)}{\partial X_i}-\frac{\partial\mathbf{S}\left(\mathbf{X}^c\right)}{\partial X_i}\cdot\Delta\boldsymbol{\alpha}\left(\mathbf{X}^c\right)\right)\right|\cdot\Delta X_i\,. \tag{28}$$

Here, the uncertainties in the natural frequencies and mode shapes are considered independent of each other. Consequently, the partial derivative of the modal data change vector and sensitivity matrix in Eqs. (27) and (28) can be calculated as follows:

$$\frac{\partial\Delta\mathbf{e}\left(\mathbf{X}^c\right)}{\partial X_i}=\frac{\partial\mathbf{e}_c\left(\mathbf{X}^c\right)}{\partial X_i}-\frac{\partial\mathbf{e}\left(\mathbf{X}^c\right)}{\partial X_i},\quad i=1,2,\ldots,nv \tag{29}$$

$$\frac{\partial S_{f_{jk}}\left(\boldsymbol{X}^c\right)}{\partial X_i}=\frac{\partial\left(\boldsymbol{\phi}_j\left(\mathbf{X}^c\right)^T\mathbf{K}_k\boldsymbol{\phi}_j\left(\mathbf{X}^c\right)\right)}{\partial X_i}=2\boldsymbol{\phi}_j\left(\mathbf{X}^c\right)^T\mathbf{K}_k\frac{\partial\boldsymbol{\phi}_j\left(\mathbf{X}^c\right)}{\partial X_i}$$

$$i=1,2,\ldots,nv\,,\quad j=1,2,\ldots,nm\,,\quad k=1,2,\ldots,m \tag{30}$$

$$\frac{\partial S_{ms_{jk}}\left(\mathbf{X}^c\right)}{\partial X_i}=\sum_{l=1}^{n}\frac{1}{\lambda_j-\lambda_l}[(\frac{\partial\boldsymbol{\phi}_l^{\mathrm{T}}}{\partial X_i})\cdot\mathbf{K}_k\boldsymbol{\phi}_j\boldsymbol{\phi}_l+\boldsymbol{\phi}_l^{\mathrm{T}}\cdot(\frac{\partial\mathbf{K}_k}{\partial X_i})\cdot\boldsymbol{\phi}_j\boldsymbol{\phi}_l+\boldsymbol{\phi}_l^{\mathrm{T}}\mathbf{K}_k\cdot(\frac{\partial\boldsymbol{\phi}_j^{\mathrm{T}}}{\partial X_i})\cdot\boldsymbol{\phi}_l+\boldsymbol{\phi}_l^{\mathrm{T}}\mathbf{K}_k\boldsymbol{\phi}_j\cdot(\frac{\partial\boldsymbol{\phi}_l}{\partial X_i})],$$

$$i=1,2,\ldots,nv\,,\quad j=1,2,\ldots,nm\,,\quad l\neq j\,. \tag{31}$$

By substituting Eqs. (29)–(31) into Eqs. (27) and (28), the interval bounds of the updated ESPs can be obtained. We note that the present method is approximate using the first-order Taylor series method. More accurate interval bounds can be achieved using the global optimization method [27], which takes more computational efforts.

4. Possibility of damage existence

The interval analysis method in the previous section can be applied to both undamaged and damaged states. Subsequently, the ESPs in the undamaged and damaged FE models can be respectively obtained as the following two interval vectors:

$$\boldsymbol{\alpha}_u^I = \left\{\alpha_{u1}^I, \alpha_{u2}^I, \ldots, \alpha_{ui}^I, \ldots, \alpha_{um}^I\right\}^T, \quad i = 1, 2, \ldots, m \tag{32}$$

$$\boldsymbol{\alpha}_d^I = \left\{\alpha_{d1}^I, \alpha_{d2}^I, \ldots, \alpha_{di}^I, \ldots, \alpha_{dm}^I\right\}^T, \quad i = 1, 2, \ldots, m \tag{33}$$

where α_{ui}^I and α_{di}^I are the intervals denoted as $\left[\underline{\alpha_{ui}}, \overline{\alpha_{ui}}\right]$ and $\left[\underline{\alpha_{di}}, \overline{\alpha_{di}}\right]$, respectively, and shown in Figure 1. It can be considered as the non-probabilistic, set-theoretic undamaged–damaged ESP intersection model. Generally, the middle value of α_{di}^I is less than that of α_{ui}^I for the damaged element. The two intervals are, however, overlapped and the entire interval of α_{di} may not be smaller than that of α_{ui} completely.

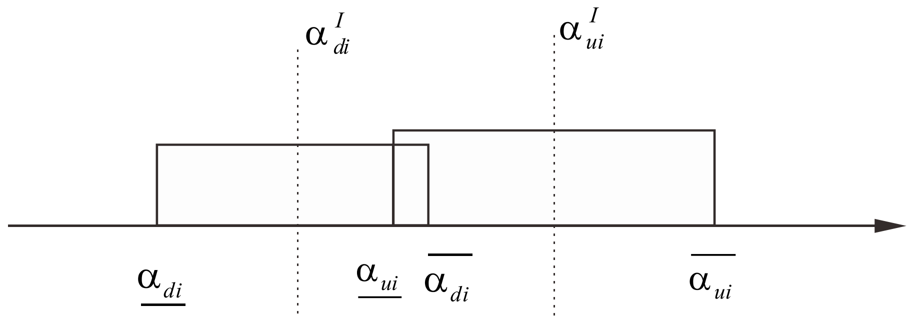

Figure 1 Illustration of ESP intervals

In this regard, a new quantitative measure of the possibility of damage existence (PoDE) is defined using the interval bounds of ESP in the undamaged and damaged states, which are respectively denoted as UESP and DESP.

Figure 2 shows the spaces of the DESP and UESP. The solid rectangle shows the possible regions of both DESP and UESP with the failure plane of *DESP = UESP*. The damage region is hatched, in which the DESP is smaller than the UESP. In this regard, the PoDE is defined as the possibility that the DESP is smaller than the UESP, which is calculated as the ratio of the area of the damage region to the total area of the basic variable region (or the rectangle), i.e.,

$$\mathrm{PoDE} = \mathrm{possibility}(\alpha_{di} < \alpha_{ui}) = \frac{A_{\mathrm{damage}}}{A_{\mathrm{total}}} \tag{34}$$

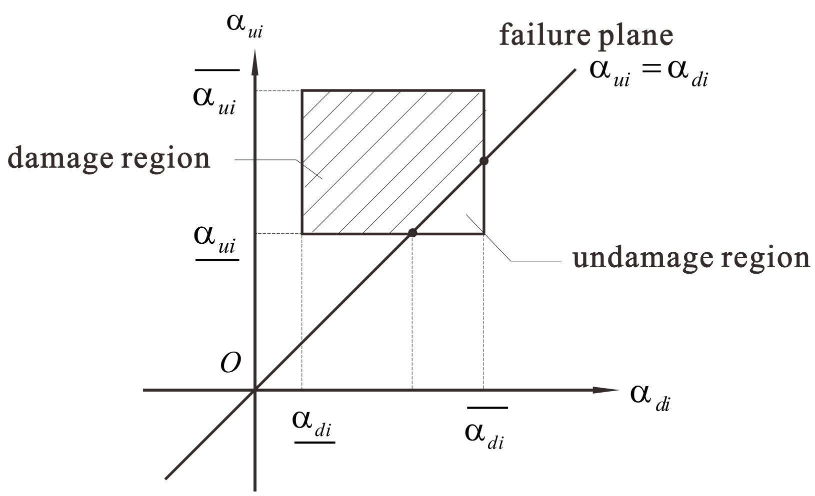

Figure 2 Space of DESP and UESP

5. Measure index for damage diagnosis

In practice, different intersection situations of the UESP and DESP may occur, as shown in Figure 3. In Figure 3(a), the distance between the middle values of the UESP and DESP is small but the two intervals separate completely, indicating a small SRF but a 100% PoDE. On the other hand, Figure 3(b) shows a large distance between the middle values of the UESP and DESP but with a significant overlapping, indicating a large SRF but a relatively small PoDE.

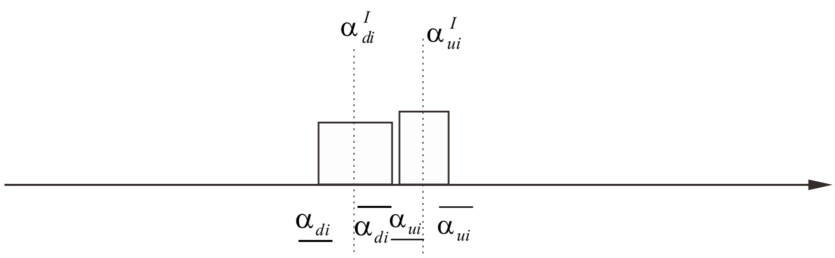

(a)

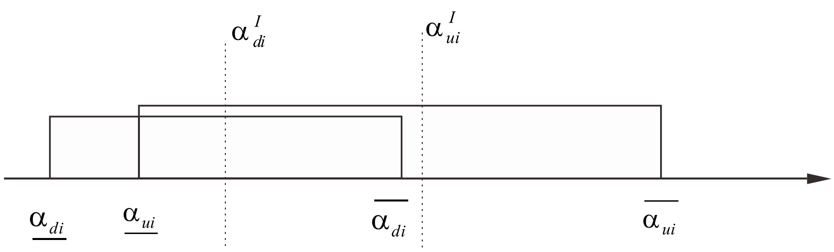

(b)

Figure 3 Intersection situations of uncertain ESPs: (a) small SRF but large PoDE, and (b) large SRF but small PoDE

Therefore, using SRF and PoDE separately may not obtain an obvious and direct damage assessment of the structure. Here, a DMI is proposed by combining SRF and PoDE. A reasonable combination would be their multiplication as

$$\beta_{\mathrm{DMI}} = \mathrm{SRF} \times \mathrm{PoDE}\,. \tag{35}$$

SRF represents the degree of damage severity whereas PoDE the possibility of damage existence. The new scalar index DMI simultaneously reflects the degree and possibility of damage of each structural element.

6. Numerical and experimental examples

A 15-bar truss structure and a laboratory-tested one-span steel portal frame are utilized to illustrate the validity of the present method in damage diagnosis.

6.1. Numerical example: 15-bar truss

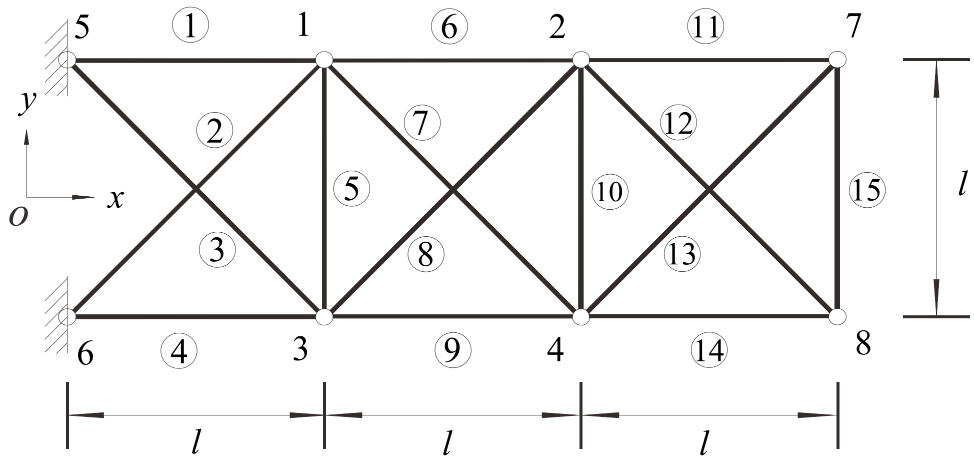

Figure 4 Schematic diagram of the 15-bar truss structure

The properties of the truss (Figure 4) are as follows: cross-sectional area A = 4×10^{-4} m^2, length l = 0.5 m, mass density of material ρ = 7.67×10^3 kg/m^3, and Young's modulus E = 2.0×10^{11} N/m^2. Here, ESP is referred to as the area of the bar element. The undamaged structure model is regarded as the initial FE model. The ESPs of element Nos. 4, 8, and 13 in the damaged structure are 25% less than the nominal ESP values in the undamaged one , i.e., $\mathrm{SRF}_{4,8,13} = -25\%$.

First, the deterministic damage identification analysis is performed by neglecting the uncertainties in the FE model and the measurement data. The SRF of each element is identified using the first eight natural frequencies and mode shapes, in which the horizontal displacements at Nos. 1, 4, 7, and 8 and the vertical displacements at Nos. 2–4 are measured. The damage identification results are shown in Figure 5. In the updating, the weights of the frequencies are considered as unity, and the weights of the mode shapes are 0.5 because the uncertainties of the mode shapes are generally greater than those of the measured frequencies in the modal testing. For comparison, the SRF of each element is also identified using the natural frequencies only and illustrated in Figure 5. The result shows that using the frequencies and mode shapes can detect correctly the damage at Nos. 4, 8, and 13, which cannot be achieved using the frequency data only.

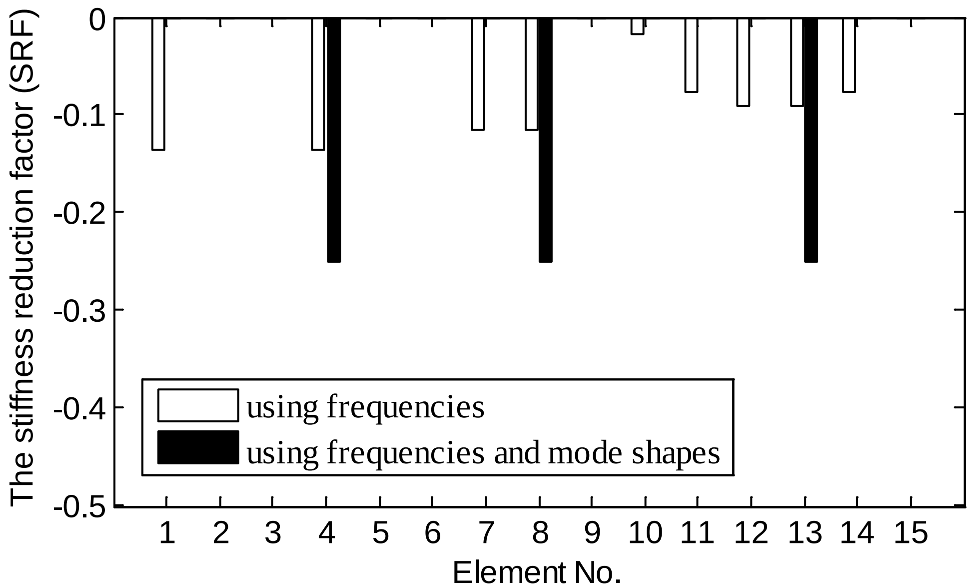

Figure 5 SRF of the truss

Next, the uncertainties of the FE model and measurement data are taken into account in the model updating. We suppose that all ESPs of the FE model have an uncertainty of 15%, and the degrees of uncertainty of the eigenvalues and mode shapes are 3% and 15%, respectively. The degree of uncertainty is defined in Eq. (19).

From the proposed interval identification method in Section 3, the intervals of the updated ESPs in the undamaged and damaged states are calculated. Figure 6 shows the interval intersection situations of the UESP and DESP identified using the first eight natural frequencies and mode shapes.

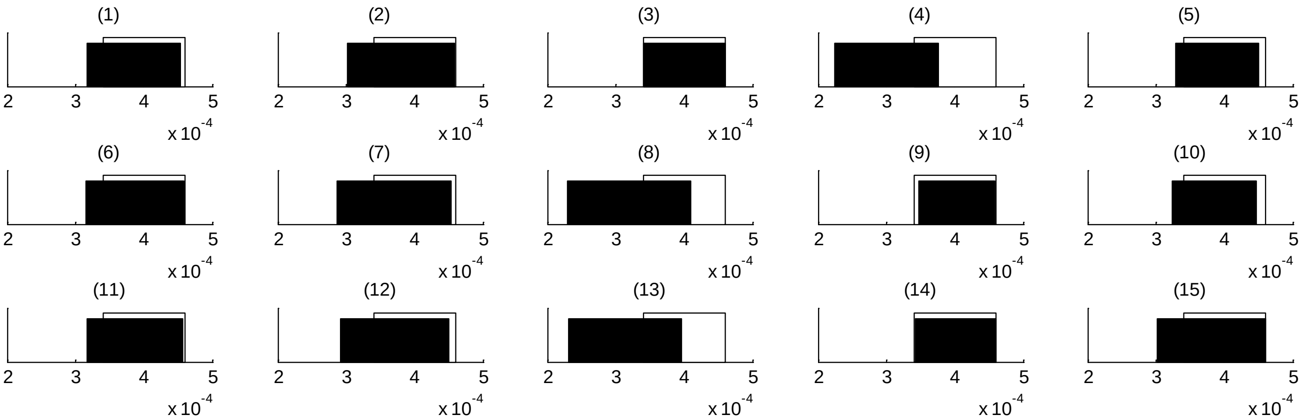

Figure 6 UESP and DESP intervals of the truss

(White bars: UESP. Black bars: DESP)

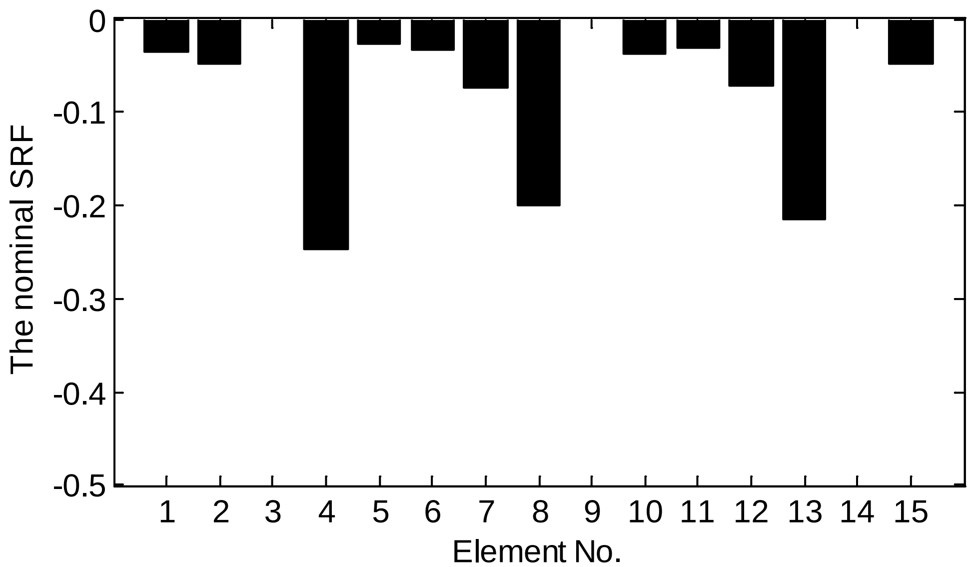

Figure 7 Nominal SRF of the truss

Figure 7 shows the nominal SRFs of all elements, indicating that the damaged elements are correctly identified. Some undamaged elements (Nos. 7 and 12) also have fair values of SRF, although not significant as the damaged one. The PoDEs of all elements are calculated by the reliability theory and listed in Table 1. The damaged elements have higher PoDE values than the undamaged ones.

Table 1 PoDE of all elements of the truss

Element No.	PoDE	Element No.	PoDE	Element No.	PoDE
1	60.4%	6	59.4%	11	58.9%
2	62.5%	7	67.6%	12	68.2%
3	49.8%	**8**	**88.5%**	**13**	**91.8%**
4	**96.3%**	9	47.3%	14	49.0%
5	58.8%	10	61.7%	15	62.1%

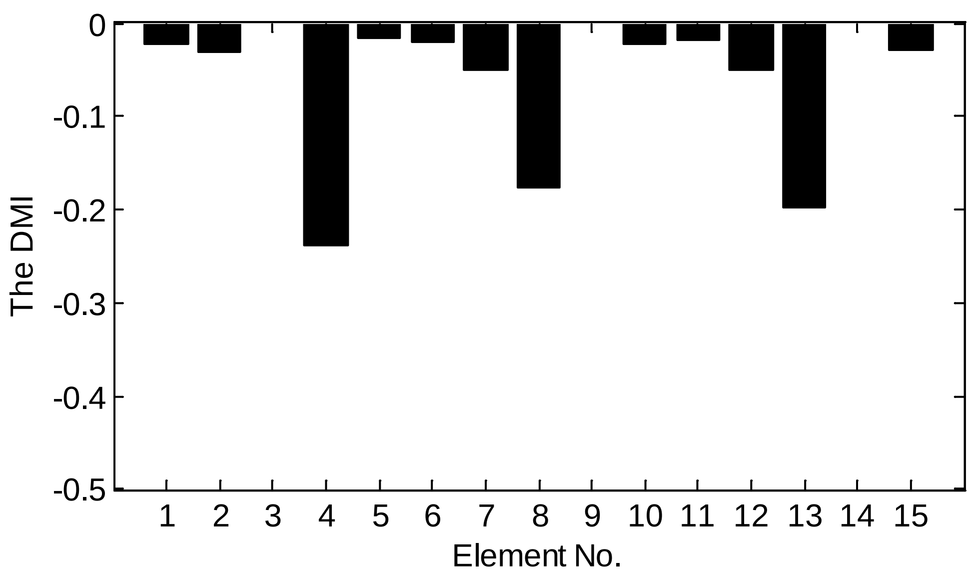

Figure 8 DMI of the truss

Figure 8 shows the DMI of the truss. The undamaged elements Nos. 7 and 12 have smaller PoDE values than the damaged elements. Therefore the undamaged and damaged elements can be easily distinguished from the proposed DMI.

The uncertainty levels of the measured data and ESPs of the analytical model may affect the structural damage identification. If the uncertainty level is too high, the true damage information may be masked by the noise and false identification results may be obtained. The effects of the uncertainty level on the DMI are investigated here.

Three uncertainty levels listed in Table 2 will be studied, where ξ_f, ξ_ϕ, and ξ_{ESP} represent the uncertainty levels of the frequency, mode shape, and ESP, respectively. The DMIs corresponding to three uncertainty levels are shown in Figure 9. It demonstrates that the damaged elements can be detected even the uncertainty level is high. In addition, higher uncertainty level, smaller difference between the DMIs of the damaged and undamaged elements, indicating that the damage can be detected more difficultly.

Table 2 Three uncertainty levels of the parameters

Case	ξ_f	ξ_ϕ	ξ_{ESP}
1	1%	5%	5%
2	3%	15%	15%
3	5%	25%	25%

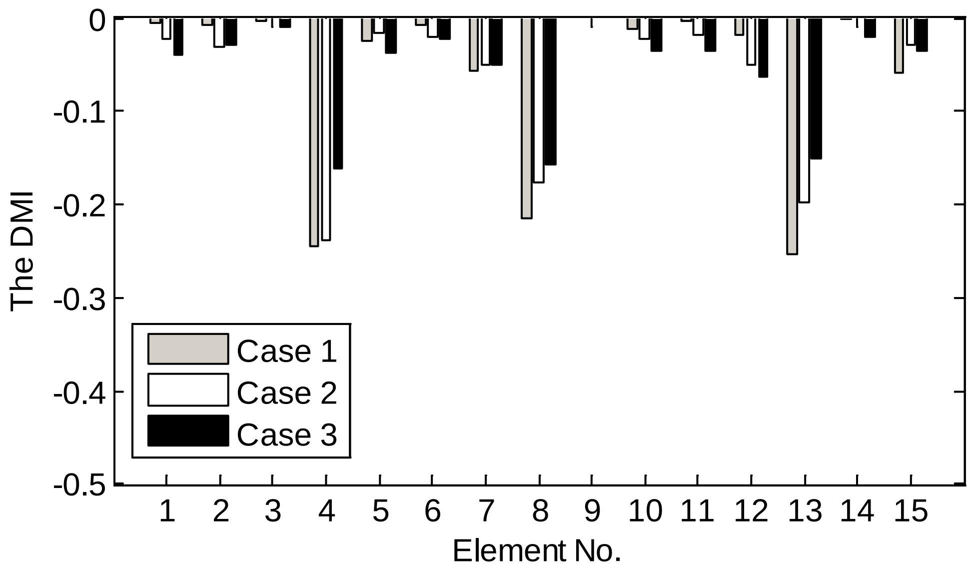

Figure 9 DMI in the three cases of uncertainty

6.2. Experimental example: one-span steel portal frame

The second example is an experimental frame shown in Figure 10. The cross section of the beam was 40.50 × 6.0 mm^2, and that of the columns was 50.50 × 6.0 mm^2. The beam and columns were welded together to simulate the rigid connection. The mass density was 7.67×10^3 kg/m^3. To test the identifiability of damages in the spatial locations, four saw cuts at different locations were made, as shown in Figure 10. Details of the experiment can be found in the works of Hao and Xia [24]. The first 12 frequencies and mode shapes were identified by the non-linear least square method [28].

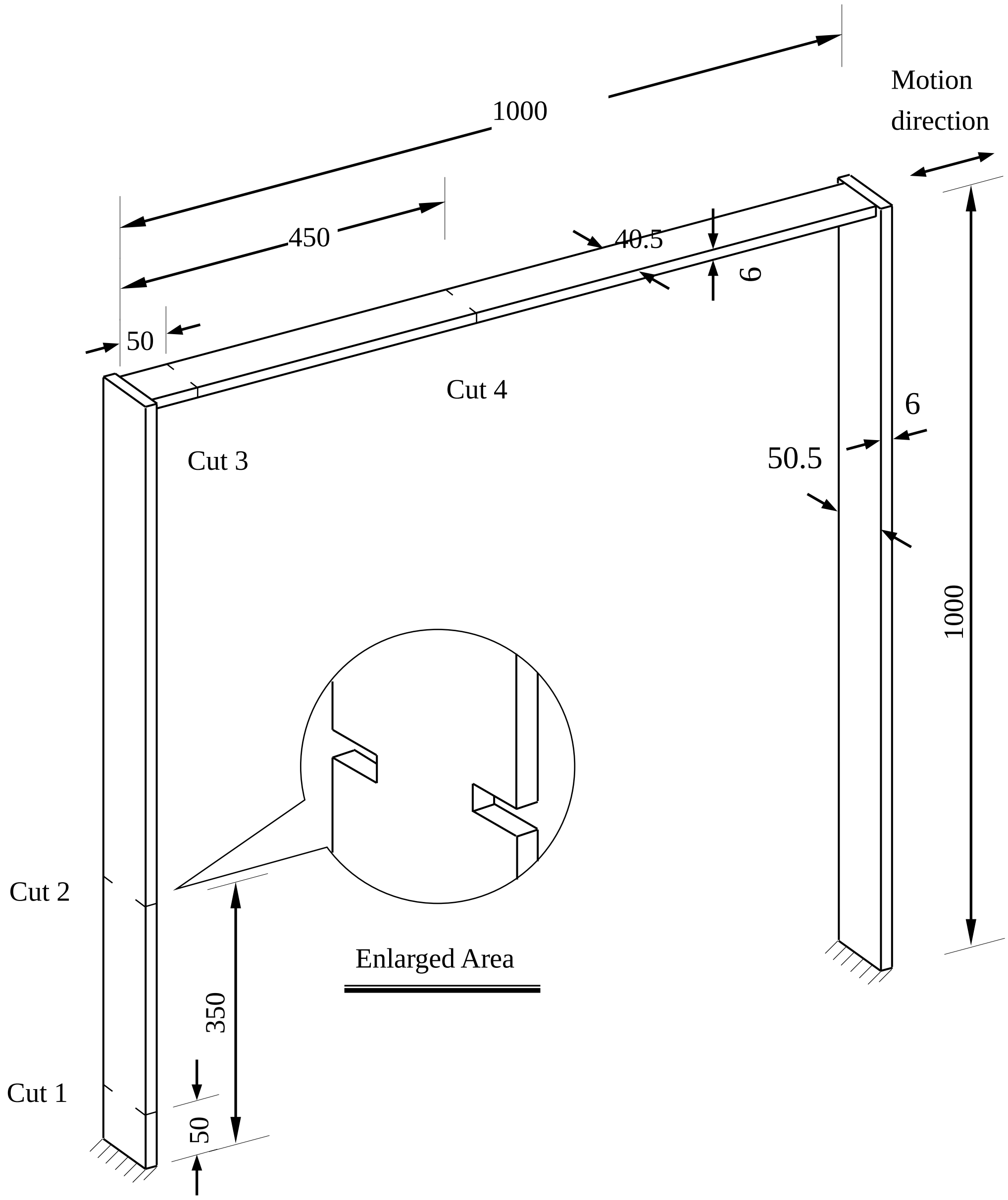

Figure 10 Configuration of the frame specimen (unit: mm)

First, the deterministic damage identification analysis is performed, in which the first 12 measured modal frequencies and mode shapes in the intact and damaged states are used to detect the artificial damages. Figure 11 shows the FE model with 30 Euler–Bernoulli beam elements (m = 30 and nm = 12). The saw cuts are located in elements 1, 4, 11, and 15. The initial Young's modulus in the intact state is estimated as 2.0×10^{11} N/m^2.

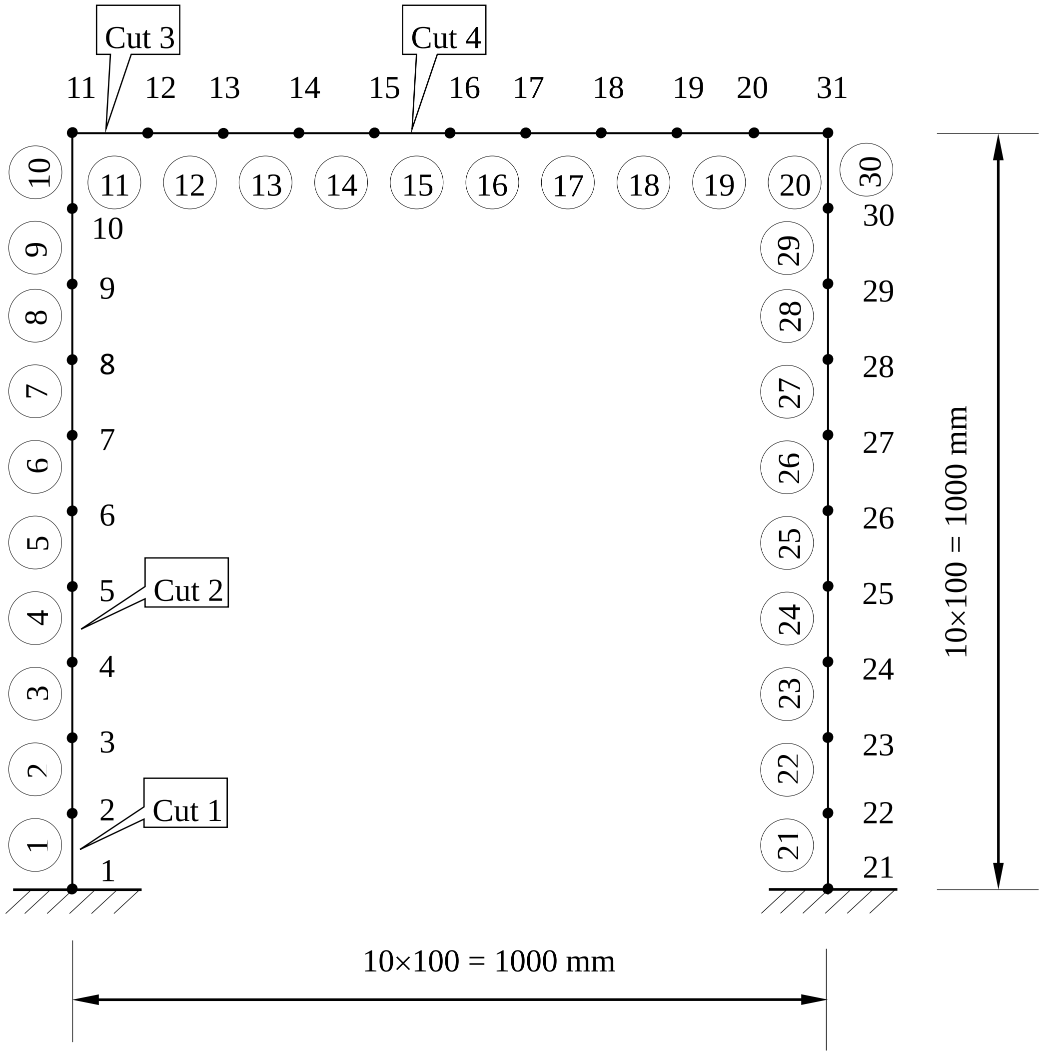

Figure 11 FE model of the frame

In the updating, the weights of the frequencies are considered as unity, and the weights of the mode shapes are regarded as 0.1. The SRFs are obtained and shown in Figure 12. Elements 1, 4, 11, and 15 have much larger SRFs than the others, indicating that damage occurs in these elements.

Next, the interval-based damage identification procedure with consideration of the measurement noise and modelling error is performed. The uncertainty intervals of the eigenvalues, mode shapes, and ESP of the FE model are assumed as 2%, 20%, and 20%, respectively.

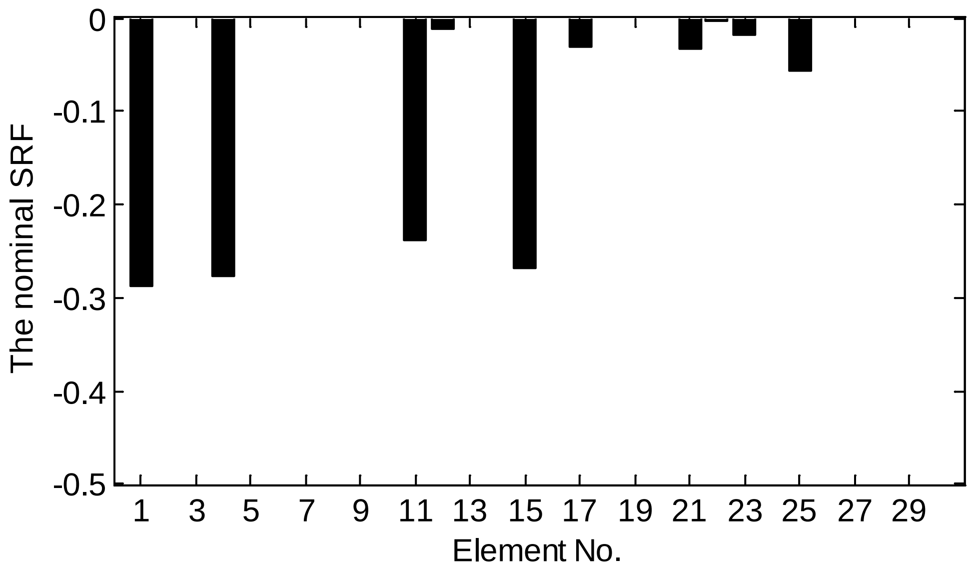

Figure 12 Nominal SRF of the frame

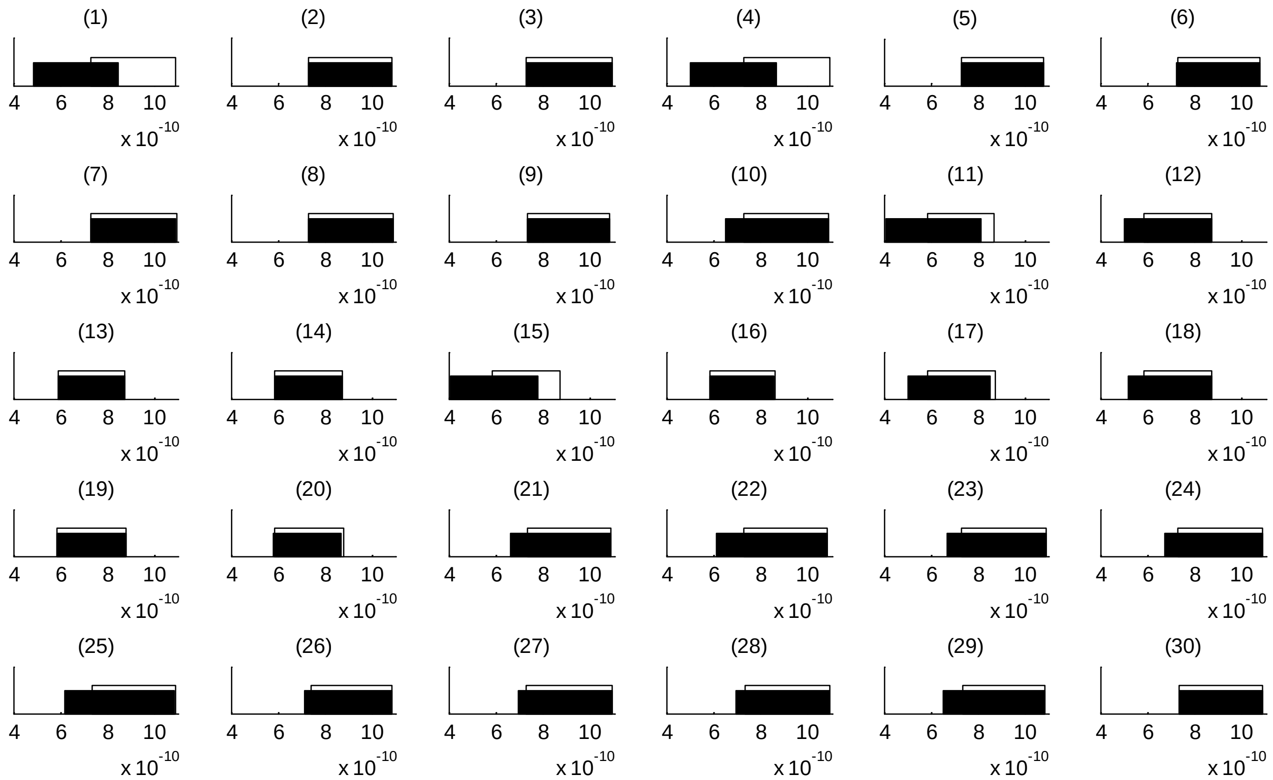

Figure 13 UESP–DESP interference of each element

(White bars: UESP. Black bars: DESP)

The intervals of the updated ESPs in the undamaged and damaged states are then calculated and shown in Figure 13. The PoDE of each element is listed in Table 3. The damaged elements have higher PoDE values than the undamaged elements. The proposed DMI of the frame are shown in

Figure 14. From the comparison between the nominal SRFs and the DMIs, the undamaged and damaged elements can be easily distinguished from Figure 14 than those from Figure 12.

Table 3 PoDE of all elements of the frame

Element	PoDE	Element	PoDE
1	**94.6%**	16	51.6%
2	50.0%	17	64.6%
3	50.1%	18	59.2%
4	**92.7%**	19	50.1%
5	50.0%	20	52.9%
6	50.6%	21	58.3%
7	50.2%	22	62.4%
8	50.0%	23	57.6%
9	50.0%	24	56.7%
10	59.2%	25	62.4%
11	**77.8%**	26	53.8%
12	61.4%	27	54.3%
13	50.0%	28	54.9%
14	50.0%	29	59.4%
15	**82.6%**	30	50.1%

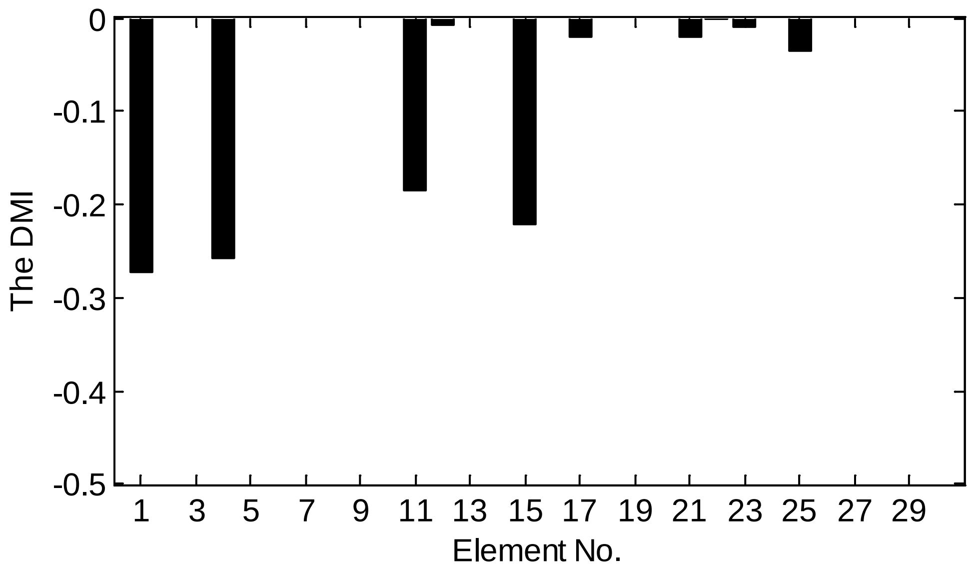

Figure 14 DMI of the frame

7. Conclusions and discussions

In this paper, both measurement noise and modelling error have been considered in structural damage identification. The statistical intervals of the structural parameters in both undamaged and damaged states have been derived using the non-probabilistic interval analysis framework. By virtue of the concept of reliability theory, a PoDE measure was developed based on the intersection set model of the undamaged and damaged structural parameters. A new damage measure index was proposed for damage diagnosis by considering both the damage severity and damage existence possibility. Numerical and experimental examples demonstrated that the damage index provides a more obvious distinction between the undamaged and damaged components. Consequently the accuracy of the damage diagnosis is improved.

In experiments and real applications, the modal parameter bounds between different modes might be correlated, so do the structural parameter bounds. However, this correlation is difficult to quantify. Their independency is thus assumed in the present paper for simplicity, that is, the modal parameters between different modes are assumed independent. More realistic uncertainty bounds deserve further study in future.

Acknowledgments

The authors would like to thank the National Nature Science Foundation of China (No. 11002013), the Aeronautical Science Foundation of China (No. 2012ZA51010), and CII (Hong Kong) / PolyU Innovation Fund (No. 5-ZJD3) for the financial supports.

References

[1] S.W. Doebling, C.R. Farrar, M.B. Prime, D.W. Shevitz, Damage identification and health monitoring of structural and mechanical systems from changes in their vibration characteristics: A literature review, Los Alamos National Laboratory Report LA-13070-MS, 1996.

[2] S.W. Doebling, C.R. Farrar, M.B. Prime, A summary review of vibration-based damage identification methods, Sage, Thousands Oaks, CA, ETATS-UNIS, 1998.

[3] G. Hearn, R. Testa, Modal analysis for damage detection in structures, Journal of Structural Engineering, 117 (1991) 3042-3063.

[4] E. Parloo, P. Guillaume, M. Van Overmeire, Damage assessment using mode shape sensitivities, Mechanical Systems and Signal Processing, 17 (2003) 499-518.

[5] B. Jaishi, W.X. Ren, Damage detection by finite element model updating using modal flexibility residual, Journal of Sound and Vibration, 290 (2006) 369-387.

[6] H. Sohn, C.R. Farrar, Damage diagnosis using time series analysis of vibration signals, Smart Materials & Structures, 10 (2001) 446-451.

[7] S. Choi, N. Stubbs, Damage identification in structures using the time-domain response, Journal of Sound and Vibration, 275 (2004) 577-590.

[8] P.E. Carden, J.M.W. Brownjohn, ARMA modelled time-series classification for structural health monitoring of civil infrastructure, Mechanical Systems and Signal Processing, 22 (2008) 295-314.

[9] Z. Sun, C. Chang, Structural damage assessment based on wavelet packet transform, Journal of Structural Engineering, 128 (2002) 1354-1361.

[10] J.T. Kim, Y.S. Ryu, H.M. Cho, N. Stubbs, Damage identification in beam-type structures: frequency-based method vs mode-shape-based method, Engineering Structures, 25 (2003) 57-67.

[11] B. Moaveni, J.P. Conte, F.M. Hemez, Uncertainty and sensitivity analysis of damage identification results obtained using finite element model updating, Computer-Aided Civil and Infrastructure Engineering, 24 (2009) 320-334.

[12] J.D. Collins, G.C. Hart, T.K. Hasselman, B. Kennedy, Statistical identification of structures, AIAA Journal, 12 (1974) 185-190.

[13] Y. Xia, H. Hao, Statistical damage identification of structures with frequency changes, Journal of Sound and Vibration, 263 (2003) 853-870.

[14] Y. Xia, H. Hao, J.M.W. Brownjohn, P.Q. Xia, Damage identification of structures with uncertain frequency and mode shape data, Earthquake Engineering & Structural Dynamics, 31 (2002) 1053-1066.

[15] X.Y. Li, S.S. Law, Damage identification of structures including system uncertainties and measurement noise, AIAA Journal, 46 (2008) 263-276.

[16] B.I. Yeo, S. Shin, H.S. Lee, S.P. Chang, Statistical damage asssessment of framed structures from static response, Journal of Engineering Mechanics, 126 (2000) 414-421.

[17] K. Zhang, H. Li, Z. Duan, S.S. Law, A probabilistic damage identification approach for structures with uncertainties under unknown input, Mechanical Systems and Signal Processing, 25 (2011) 1126-1145.

[18] S. Gabriele, C. Valente, F. Brancaleoni, An interval uncertainty based method for damage identification, Key Engineering Materials, 347 (2007) 551-556.

[19] O. García, J. Vehí, J. Campos e Matos, A. Abel Henriques, J. Ramon Casas, Structural

assessment under uncertain parameters via interval analysis, Journal of Computational and Applied Mathematics, 218 (2008) 43-52.
[20] X.J. Wang, H.F. Yang, Z.P. Qiu, Interval analysis method for damage identification of structures, AIAA Journal, 48 (2010) 1108-1116.
[21] X.J. Wang, H.F. Yang, L. Wang, Z.P. Qiu, Interval analysis method for structural damage identification based on multiple load cases, Journal of Applied Mechanics, 79 (2012) 051010-051018.
[22] X.J. Wang, Z.P. Qiu, I. Elishakoff, Non-probabilistic set-theoretic model for structural safety measure, Acta Mechanica, 198 (2008) 51-64.
[23] R.L. Fox, M.P. Kapoor, Rate of change of eigenvalues and eigenvectors, AIAA Journal, 6 (1968) 2426-2429.
[24] H. Hao, Y. Xia, Vibration-based damage detection of structures by genetic algorithm, Journal of Computing in Civil Engineering, 16 (2002) 222-229.
[25] Z.P. Qiu, X.J. Wang, Comparison of dynamic response of structures with uncertain-but-bounded parameters using non-probabilistic interval analysis method and probabilistic approach, International Journal of Solids and Structures, 40 (2003) 5423-5439.
[26] H.Y. Liu, Reliability Analysis of Structures Under Explosive Loading, Master Thesis, Nanyang Technological University, Singapore, 2001.
[27] E. Hansen, G.W. Walster, Global Optimization Using Interval Analysis: Revised And Expanded, Taylor & Francis, 2003.
[28] N.M.M. Maia, J.M.M. Silva, J. He, N.A.J. Lieven, R.M. Lin, G.W. Skingle, W. To, A.P.V. Urgueira, Theoretical and Experimental Modal Analysis, Taylor & Francis, 1997.

List of figures